# Dynamic behavior of two neighboring nanobubbles induced by various gas-liquid-solid interactions

Chenliang Li,[1] Shi-Ping Wang,[2,*] A-Man Zhang,[2,*] and Yunlong Liu[2]
[1]*College of Aerospace and Civil Engineering, Harbin Engineering University, Harbin 150001, People's Republic of China*
[2]*College of Shipbuilding Engineering, Harbin Engineering University, Harbin 150001, People's Republic of China*

(Received 5 May 2018; published 26 December 2018)

We systematically investigate the dynamic behavior of two neighboring nanobubbles for various gas-liquid-solid interactions by molecular dynamics simulations. The weaker the interaction between gas and liquid, the larger are the bulk nanobubbles formed. The dynamic behavior of bulk nanobubbles depends not only on the ratio of gas-gas to liquid-gas interaction strengths, but also on that of solid-gas to liquid-gas interaction strengths. A very small bulk nanobubble remains stable in bulk liquid, as long as the ratio of solid-gas to liquid-gas interaction strengths is sufficiently large. Under the condition that the three-phase contact line is not pinned, different dynamic behaviors of two neighboring surface nanobubbles are observed. For a higher ratio of solid-gas to solid-liquid interaction strengths, the two neighboring surface nanobubbles can merge directly owing to the existence of a film layer of gas molecules between them. This film layer allows transfer of gas molecules from one surface nanobubble to the other along the solid substrate. This result is consistent with other theoretical results. If the interaction between solid and gas is sufficiently strong, two neighboring unsaturated surface nanobubbles can form a gas-rich layer on the solid surface. The formation of such a layer is very important for effective weakening of the solid-liquid interaction, leading to a greater reduction in drag. The effect of the ratio of solid-gas to solid-liquid interaction strengths on the shape of the gas-rich layer is also discussed in detail.

DOI: 10.1103/PhysRevFluids.3.123604

## I. INTRODUCTION

For both underwater and surface marine vehicles, frictional resistance is the main cause of increased energy consumption and reduced travel speed, and indeed it contributes a large proportion of the total resistance. Therefore, finding methods to effectively reduce frictional resistance on marine vehicles and thereby increase travel speed is an important problem. As is well known, an object moving in water is subject to a larger drag force than in air because of the greater dynamic viscosity of water [1]. This is the motivation behind the proposal that frictional drag on vehicles moving in water could be reduced by replacing the solid-liquid interface by a solid-gas interface [2,3]. Some studies have already demonstrated that an air layer or bubble mattress covering a vehicle moving in water can provide a reduction in frictional drag by 25–80% [4–8]. Consequently, many investigations have been carried out to explore the formation and behavior of air layers and bubbles in solid-liquid interfaces.

*Corresponding authors: wangshiping@hrbeu.edu.cn; zhangaman@hrbeu.edu.cn

 

Nanobubbles are nanoscopic gas bubbles that can be produced on interfaces (surface nanobubbles) or in bulk solutions (bulk nanobubbles) [9]. The stability and growth mechanisms of single surface nanobubbles have been extensively investigated both experimentally and theoretically. These studies have shown that on the nanoscale, nanobubbles exhibit some extraordinary properties, such as longer lifetime, larger specific surface, smaller rise speed, and slower dissolution than expected [10]. For example, Weijs *et al.* [11] analyzed the formation and stability of a single surface nanobubble in simple fluids using molecular dynamics (MD) simulation. It was found that surface nanobubbles can survive for more than a day rather than the expected microseconds [12]. Maheshwari *et al.* [13] and Wei *et al.* [14] further studied the effects of the solid surface and gas oversaturation on the stability and growth of a single surface nanobubble. Although these studies are important with regard to the development of nanobubbles, it should be noted that such bubbles do not occur singly in most cases, but rather exist in the neighborhood of other nanobubbles [15,16]. Therefore, it is necessary to investigate interactions between nanobubbles.

In an experimental investigation, Bhushan *et al*. [17] and Li *et al.* [18] studied the movement and coalescence of two surface nanobubbles on a solid-liquid interface using tapping mode atomic force microscopy. Detailed observations of the process of the merger of surface nanobubbles were obtained. Bhushan *et al.* [17] found that small nanobubbles move faster and merge into larger ones. However, according to Li *et al.* [18], there is uncertainty regarding whether a larger or smaller nanobubble will move first to merge into others. The reason is that both the contact line and surface properties could affect the merger process. Park *et al.* [19] investigated distortions in the shape of merging nanobubbles in a two-nanobubble system. Their results showed that the structural distortion of merging nanobubbles can be attributed to the relative size difference. Furthermore, Lohse and Zhang gave an overview on nanobubbles and potential issues in some of the experimental studies [20]. This overview is very useful to improve the development of nanobubbles.

From a theoretical viewpoint, Li *et al.* [10] studied the coalescence and movement of nanobubbles on a graphene surface in water using a MD simulation method. Their results showed that differences in the type and concentration of the gas clearly affect the formation and coalescence of nanobubbles. On the other hand, a study by Dollet and Lohse [21] showed that two nanobubbles can remain stable when the distance between them is larger than their lateral size. However, Zhu *et al.* [16] found that two neighboring nanobubbles can also remain stable even when they are very close to each other, owing to pinning and oversaturation. Motivated by these opposite results, Maheshwari *et al.* [15] further investigated the stability of two neighboring nanobubbles on a nanoscopic level using MD simulations. Their results showed that as long as the gas-solid interaction is weaker than the liquid-solid interaction, a two-nanobubble system can remain stable. From these studies, it can be seen that many different factors will affect the stability, growth, and shrinkage of a multiple-nanobubble system. This has stimulated us to study such systems further. Moreover, such studies are essential to further extend the potential applications of nanobubbles.

In this paper, the effect of various gas-liquid-solid interactions on the dynamic behavior of a multiple-nanobubble system is investigated using MD simulations. We study not only a system with multiple surface nanobubbles, but also one with multiple bulk nanobubbles. The results suggest that the size of bulk nanobubbles can be effectively controlled by various gas-liquid interactions. A large bulk nanobubble has the ability to absorb other bulk nanobubbles in bulk liquid. It is found that two neighboring surface nanobubbles exhibit two types of dynamic behavior under certain conditions. It is interesting to find that two neighboring unsaturated surface nanobubbles can also form a gas-rich layer on a solid surface, as long as the interaction between the solid and the gas is sufficiently strong.

## II. SIMULATION METHODOLOGY

MD simulations were performed in a 9.84 nm $\times$ 17.04 nm $\times$ 8 nm simulation box using the open source GROMACS software package [22]. We used three types of molecules in our simulations: a solid graphene molecule ($s$), $N_2$ and $O_2$ gas molecules ($g$), and liquid molecules ($l$). $N_2$ and $O_2$ are the main ingredients of air, and these molecules are simulated using a united atom model. The liquid

TABLE I. Values of the Lennard-Jones parameters used in the MD simulations.

| $i$-$j$ | $\sigma_{ij}$ (nm) | $\varepsilon_{ij}$ (kJ/mol) |
|---|---|---|
| $s$-$l$ | 0.32 | 1.7, 1.6, 1.5, 1.4, and 1.3 |
| $s$-$g$ | 0.4 | 2.0 |
| $l$-$g$ | 0.4 | 1.5, 1.45, 1.40, and 1.35 |
| $g$-$g$ | 0.32 | 0.79 |
| $l$-$l$ | 0.48 | 2.85, 2.66, 2.48, and 2.31 |

phase is represented by a water model. Firstly a *NVT* and *NPT* were done to ensure that the system was equilibrated, and then all simulations were performed under a *NPT* ensemble.

The interaction between the molecules is described by the Lennard-Jones (LJ12-6) potential,

$$V_{\mathrm{LJ}}(r_{ij}) = 4\varepsilon_{ij}\left[\left(\frac{\sigma_{ij}}{r_{ij}}\right)^{12} - \left(\frac{\sigma_{ij}}{r_{ij}}\right)^{6}\right], \tag{1}$$

where $\varepsilon_{ij}$ and $\sigma_{ij}$ are, respectively, the interaction strength and range between atoms $i$ and $j$. The complete set of Lennard-Jones parameters for various solid-liquid, solid-gas, and liquid-gas interactions is given in Table I. A 1.5-nm cutoff length was used for the Lennard-Jones potential function. A time step of 2 fs was used to update the molecular velocities and positions, and the whole simulation time was set to be 50 ns [23]. The temperature was fixed at 300 K so that both $N_2$ and $O_2$ were in the gaseous state. A *V*-rescale thermostat was used to maintain constant temperature, and its stochastic term ensured a proper canonical ensemble [22]. Periodic boundary conditions were applied in the $x$, $y$, and $z$ directions.

We used the initial configuration as shown in Fig. 1(a) at 0 ns. Single-layer graphene as a solid substrate was fixed at its initial position throughout the simulations. The liquid molecules were arranged above the solid substrate, and the gas molecules were randomly distributed in the bulk liquid. Figure 1(b) presents a surface nanobubble on a homogeneous graphene solid surface, that is, without contact line pinning. Energy minimization was first performed using the steepest descent method. Then the final configuration of energy minimization was used in the following dynamic simulations. Quantities such as the lateral size and height of nanobubbles were evaluated by fitting the nanobubble profiles as circular arcs. The liquid-gas interface of nanobubbles is defined as the location at half the normalized density field $\rho^*(r) = \frac{\rho(r)-\rho_G}{\rho_L-\rho_G}$, where $\rho_L$ and $\rho_G$ are the bulk liquid and gas density, respectively [13–15]. Data for density were collected by averaging over 1000 output configurations separated by $1\times10^5$ simulation steps.

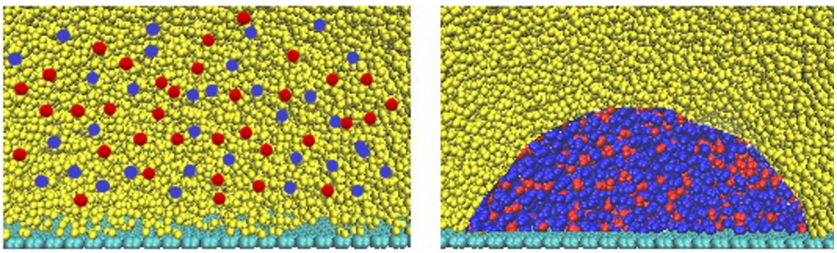


FIG. 1. (a) Initial configuration; (b) a surface nanobubble at 10 ns. Red and blue particles represent the gas phase (oxygen and nitrogen, respectively), green particles represent the solid phase, and yellow particles represent the liquid phase.

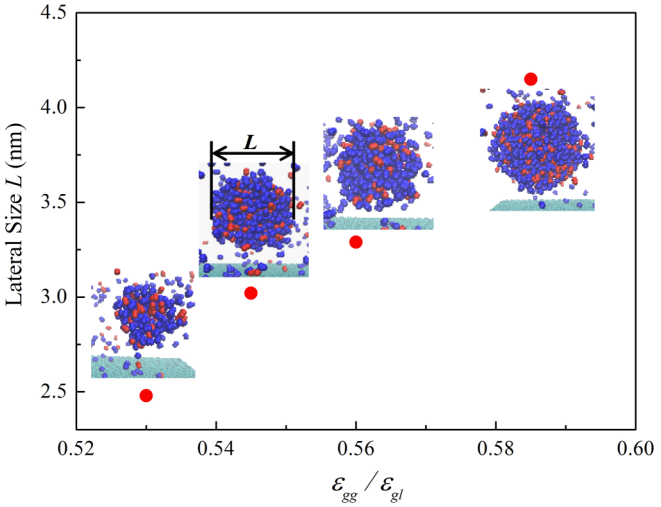


FIG. 2. Dependence of the size of bulk nanobubbles on the ratio $\varepsilon_{gg}/\varepsilon_{gl}$.

## III. RESULTS AND DISCUSSION

### A. Bulk nanobubble and surface nanobubble interactions

To date, much research effort has been dedicated to surface nanobubbles, while bulk nanobubbles have been much less widely studied although Zhang and Seddon [9] investigated the interaction of bulk nanobubble suspensions with nanoparticles, and their results suggested that bulk nanobubbles could be used to enhance scavenging effects and for surface modification. It is therefore necessary to further study the formation, growth, and dissolution of bulk nanobubbles. The formation of bulk nanobubbles requires higher gas concentrations than the formation of surface nanobubbles. In previous work, we have demonstrated that when the gas concentration in the bulk liquid is above 3.5%, bulk nanobubbles can be generated [10]. Therefore, in the present study, the gas concentration was fixed at 7.3%. The spontaneous formation of surface nanobubbles can be attributed to a combination of gas oversaturation and a hydrophobic solid surface. Gas oversaturation was reached when the gas concentration was fixed at 7.3%. Meanwhile, the graphene is strongly hydrophobic, which means that the solid-gas interaction is stronger than the solid-liquid interaction. As a result, a graphene surface strongly attracts gas molecules, leading to spontaneous formation of surface nanobubbles.

In this work, by increasing the strength of the gas-gas interaction relative to the strengths of the other interactions, bulk nanobubbles of different lateral size $L$ were generated. Figure 2 shows the effect of the ratio of the gas-gas to gas-liquid interaction strengths ($\varepsilon_{gg}/\varepsilon_{gl}$) on the size of bulk nanobubbles. The weaker the interaction between gas and liquid, the greater is the size of the bulk nanobubbles formed. The reason is that the change of $\varepsilon_{gg}/\varepsilon_{gl}$ influences the solubility of gas in liquid which changes the gas oversaturation in bulk liquid, leading to the change of nanobubble size. Further studies have shown that larger bulk nanobubbles are more stable than smaller ones. To illustrate this more clearly, in Fig. 3(a), we plot the number of gas molecules in a single bulk nanobubble as a function of time for two different values of the ratio $\varepsilon_{gg}/\varepsilon_{gl}$. Figure 3(a) reveals the dynamic process of growth and dissolution of bulk nanobubbles. It can be seen that several gas molecules first come together to form a small nucleation point that constantly absorbs surrounding gas molecules, thereby forming a bulk nanobubble. Under the condition of strong gas-liquid interaction ($\varepsilon_{gg}/\varepsilon_{gl} = 0.53$), a small bulk nanobubble is formed, including only a few gas molecules (about 200). This small bubble is highly unstable, and it gradually dissolves as a result of outflow of gas molecules into the bulk liquid. In contrast, with weak gas-liquid interaction

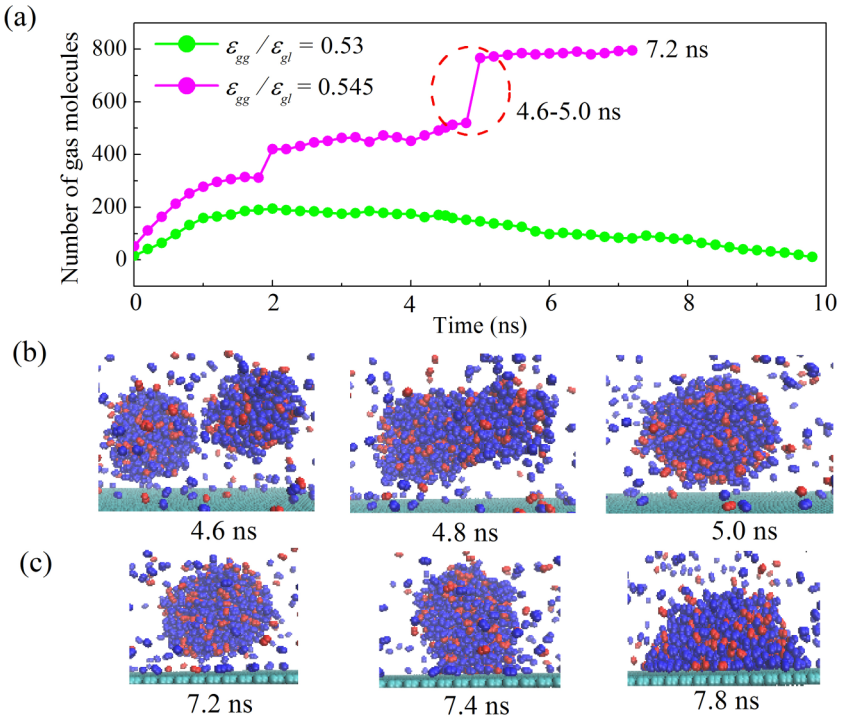


FIG. 3. (a) Dynamic process of growth and dissolution of a bulk nanobubble; (b) interaction between two neighboring bulk nanobubbles; (c) dynamic process of transformation of a bulk nanobubble into a surface nanobubble.

($\varepsilon_{gg}/\varepsilon_{gl} = 0.545$), a large bulk nanobubble is formed and remains stable. Meanwhile, sudden jumps are observed in the number of gas molecules at 2.2 and 4.9 ns. The reason is that a large bulk nanobubble grows by absorbing surrounding bulk nanobubbles, as shown in Fig. 3(b). According to Henry's law and Laplace's equation, the concentration of gas around a smaller bulk nanobubble is greater than that around a larger one. Therefore, a strong concentration gradient is present in the system, and this can facilitate transfer of gas molecules from one nanobubble to another, inducing coalescence of a large bulk nanobubble with surrounding bulk nanobubbles.

A growing large bulk nanobubble cannot stay in the bulk liquid forever, and two types of dynamic behavior are observed under certain conditions. In one type, bubble growth eventually slows down on the solid surface owing to the highly hydrophobic nature of the surface, and the bulk nanobubble becomes a surface nanobubble. Figure 3(c) shows this transformation of a bulk nanobubble into a surface nanobubble. As mentioned earlier, a small bulk nanobubble with about 200 gas molecules (and with lateral size $L = 2.48$ nm) dissolves into the bulk liquid, as shown by the green line in Fig. 3(a). However, Li *et al.* [10] showed that a very small bulk nanobubble, containing only 125 gas molecules (and with lateral size $L = 1.8$ nm), could also remain stable in bulk liquid. The small bulk nanobubble was observed to sink, finally falling onto the solid surface. To explain these opposing results, we compared the strengths of gas-liquid-solid interactions. We found that the value of $\varepsilon_{sg}/\varepsilon_{gl}$ in our simulation was lower than that in the studies by Li *et al.* The strength of the solid-gas interaction was high compared with that of the liquid-gas interaction, leading to the movement of the small bulk nanobubble toward the solid surface. During this movement, the small nanobubble did not dissolve in the bulk liquid, owing to the relatively weak liquid-gas interaction. Therefore, the dynamic behavior of a bulk nanobubble is related not only to $\varepsilon_{gg}/\varepsilon_{gl}$ but also to $\varepsilon_{sg}/\varepsilon_{gl}$.

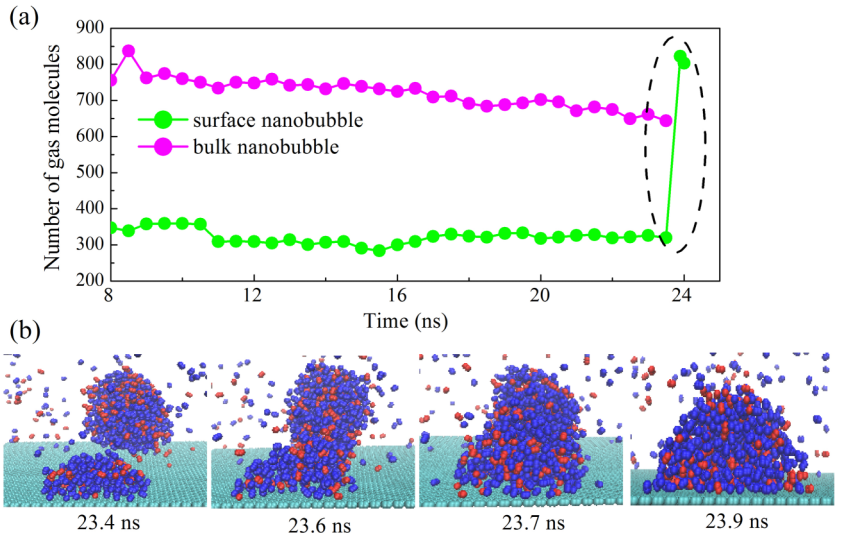


FIG. 4. Interaction between a bulk nanobubble and a surface nanobubble, (a) variation of number of gas molecules; (b) dynamic process of interaction between a bulk nanobubble and a surface nanobubble.

In the second type of behavior, as shown in Fig. 4(a), a bulk nanobubble merges directly with a nearby surface nanobubble. The bulk nanobubble is almost stable owing to the weak gas-liquid interaction. At 23.4 ns, the bulk nanobubble starts to merge with the nearby surface nanobubble in the bulk liquid under the condition of strong gas-gas interaction ($\varepsilon_{gg}/\varepsilon_{gl} = 0.585$). Before merging, the radius of the surface nanobubble (4.42 nm) is greater than that of the bulk nanobubble (3.61nm). As a result, the surface nanobubble is more stable than the bulk nanobubble. Moreover, the stable surface nanobubble on the graphene solid looks like a gas nucleation point that absorbs the surrounding bulk nanobubble, leading to a net flux of gas molecules from bulk nanobubbles to surface nanobubbles through the bulk liquid. Figure 4(b) clearly shows this flow of gas molecules from the bulk nanobubble to the surface nanobubble, inducing distortion of the bulk nanobubble toward the surface nanobubble. As a result, the number of gas molecules in the surface nanobubble exhibits a sudden jump at 23.9 ns in Fig. 4(a). On the basis of these results, it can be concluded that the dynamic behavior of bulk nanobubbles depends strongly on the gas-solid-liquid interactions, as well as on the gas concentration.

### B. Interaction between two neighboring surface nanobubbles

The interaction between two neighboring surface nanobubbles differs from that between a bulk nanobubble and a surface nanobubble. Owing to the absence of a three-phase contact line, the bulk nanobubble usually either dissolves or transforms into a surface nanobubble. A recent theoretical study has shown that two neighboring surface nanobubbles can remain stable and not interact, as long as the gas-solid interaction is weak compared with the liquid-solid interaction [15]. To further explore the interaction of two neighboring surface nanobubbles, we investigated their behavior for different values of the ratio of $\varepsilon_{sg}/\varepsilon_{sl}$. We found that there are two types of interaction behavior when the contact line is not pinned: One corresponds to the coalescence of the two surface nanobubbles into a larger nanobubble, and the other to the growth of one nanobubble at the expense of the other.

Figure 5 shows the number of gas molecules $N$, the lateral length $L$, and the height $H$ of the two nanobubbles as functions of time for two values of $\varepsilon_{sg}/\varepsilon_{sl}$. The two neighboring surface nanobubbles exhibit two types of interaction behavior. Figure 5(a) shows their direct merger into a large surface nanobubble for $\varepsilon_{sg}/\varepsilon_{sl} = 1.25$. Sudden jumps are observed in the number of gas

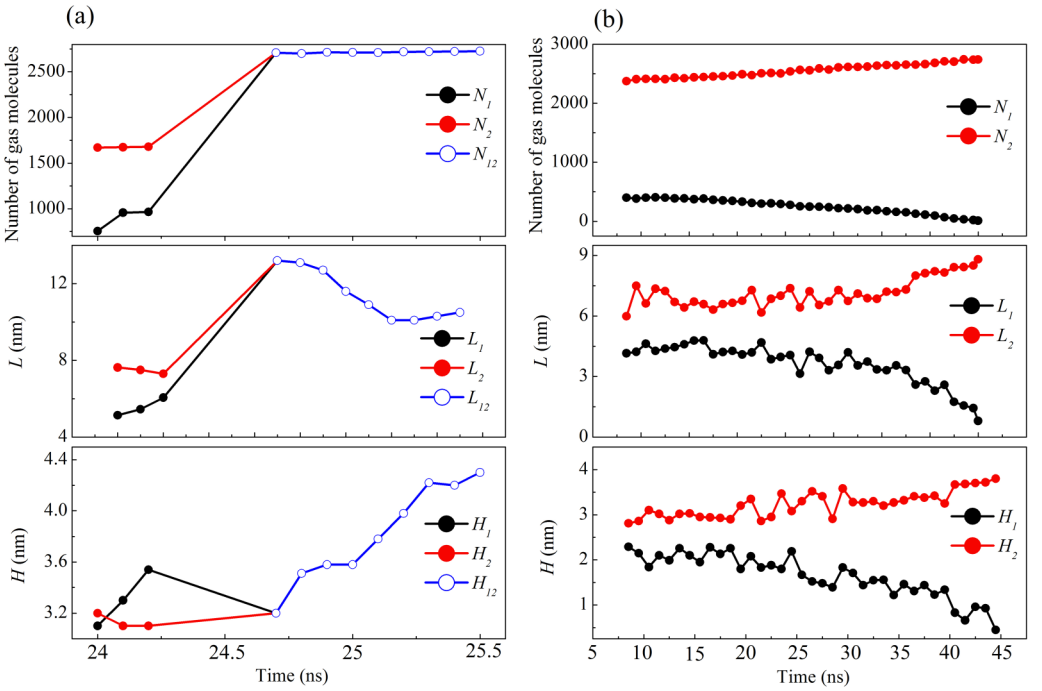


FIG. 5. Variation with time of the number of gas molecules $N$ and of the lateral size $L$ and height $H$ of two neighboring surface nanobubbles with time for (a) $\varepsilon_{sg}/\varepsilon_{sl} = 1.25$ and (b) $\varepsilon_{sg}/\varepsilon_{sl} = 1.538$. $N_i$, $L_i$ and $H_i (i = 1, 2)$ are the shape parameters of two surface nanobubbles before coalescence; $N_{12}$, $L_{12}$, and $H_{12}$ are the shape parameters after coalescence.

molecules and in the lateral lengths and the radii of the two nanobubbles between 24.2 and 24.7 ns. This means that the two surface nanobubbles can remain stable and do not dissolve before coalescence (before 24.2 ns). At 24.2 ns, the lateral lengths of the two surface nanobubbles are almost equal, and the distance between them is 0.75 nm. After this, they start to merge.

Figure 6 shows the process of the merger of two neighboring surface nanobubbles between 24.2 and 24.7 ns for $\varepsilon_{sg}/\varepsilon_{sl} = 1.538$. It can be seen that a film layer of gas molecules between two surface nanobubbles is formed on the solid surface. This film layer has the appearance of a "bridge" connecting the two neighboring surface nanobubbles. Through this bridge, gas molecules can transfer from one nanobubble to the other along the solid surface. According to Maheshwari *et al.* [13], the film layer of gas molecules is formed as a result of the strong interaction between gas and solid. It should also be noted that the lateral length $L$ after coalescence (at 24.7 ns) is exactly the sum of the lateral lengths of the two neighboring surface nanobubbles before coalescence (at 24.2 ns). This also demonstrates that the two neighboring surface nanobubbles remain stable before coalescence. After coalescence, the lateral length $L$ gradually decreased, which can be explained by free-energy considerations: Minimization of free energy requires minimization of interface area.

For $\varepsilon_{sg}/\varepsilon_{sl} = 1.538$, two surface nanobubbles are formed at 8.5 ns. As can be seen from Fig. 5(b), there are great differences in the number of gas molecules $N$, the lateral length $L$, and the height $H$. Owing to the absence of contact line pinning, the two surface nanobubbles cannot remain stable. The small nanobubble $N_2$ gradually dissolves and disappears, while the large nanobubble $N_2$ gradually grows as a result of absorption of gas molecules originating from the dissolution of the small nanobubble in a process similar to Ostwald ripening. According to free-energy considerations, a single-bubble state is more energetically favorable than a two-bubble state. In order to reach the energetically favorable state, one of the two bubbles has to overcome the three-phase contact

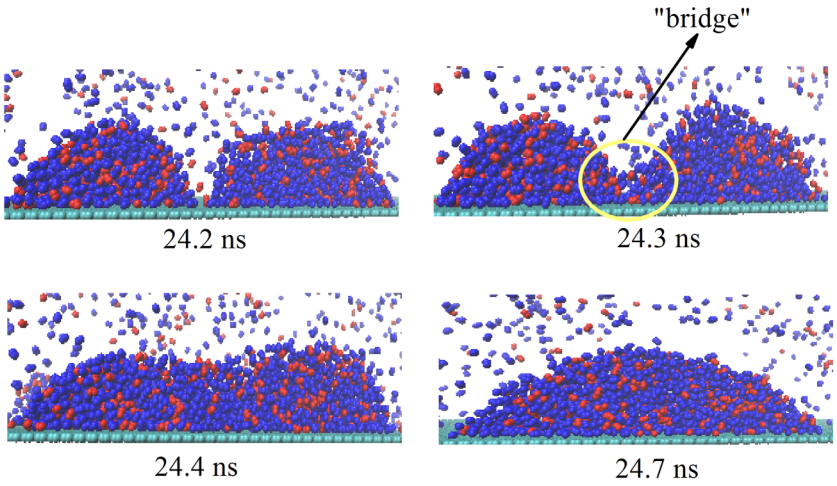


FIG. 6. Merger of two neighboring surface nanobubbles for $\varepsilon_{sg}/\varepsilon_{sl} = 1.538$.

line barrier, which requires the presence of a concentration gradient [15]. When the radius of curvature of one surface nanobubble is large compared with that of the other, this generates a strong concentration gradient, inducing a net flux of gas molecules in the bulk liquid from the small nanobubble to the large one. Therefore, the large surface nanobubble grows at the expense of the small one.

We also calculated the distance between two surface nanobubbles before coalescence; see Fig. 7. For $\varepsilon_{sg}/\varepsilon_{sl} = 1.25$, the two surface nanobubbles have similar sizes, and they move close to each other. They then start to merge through a bridge (see Fig. 6) when the distance between them decreases to 0.75 nm. For $\varepsilon_{sg}/\varepsilon_{sl} = 1.538$, the bubbles differ considerably in size, and although they also move toward each other, with a separation of about 0.75 nm at 23 ns, they do not merge. Instead, the distance between them then increases with dissolution of the small nanobubble. Although the interaction energy between gas and solid is increased, a film layer of gas molecules (bridge) between the two surface nanobubbles is not observed when $\varepsilon_{sg}/\varepsilon_{sl} = 1.538$. Growth of the large surface

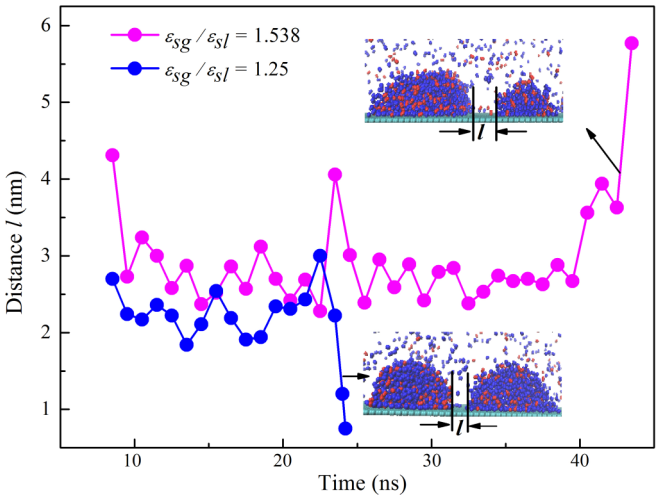


FIG. 7. Distance between two surface nanobubbles for different values of $\varepsilon_{sg}/\varepsilon_{sl}$.

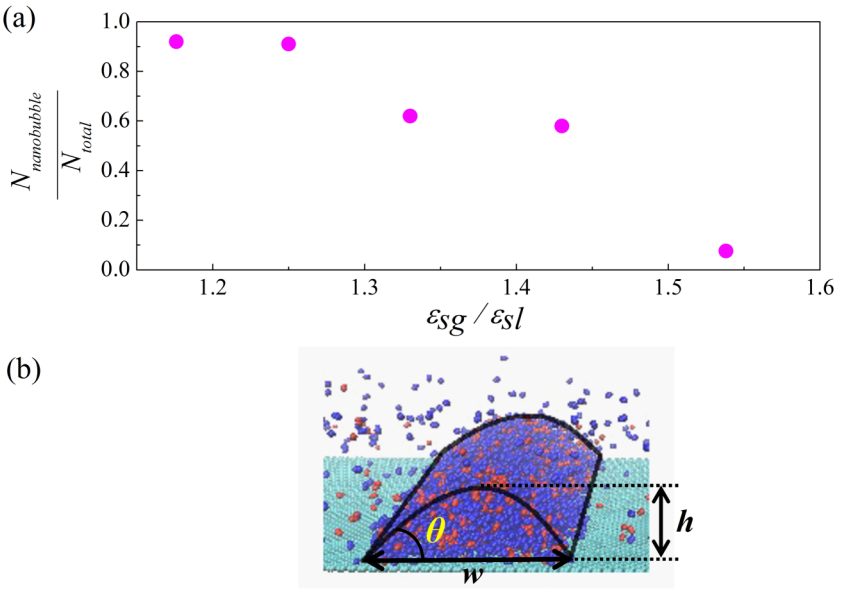


FIG. 8. (a) Gas concentration in a nanobubble required for formation of a gas-rich layer for different values of $\varepsilon_{sg}/\varepsilon_{sl}$; (b) shape of the gas-rich layer.

nanobubble can occur by absorption of gas molecules released from the small nanobubble during its dissolution. Consequently, in addition to the gas-solid interaction, both the relative size difference and the distance between two surface nanobubbles are also important in determining the interaction behavior of two neighboring surface nanobubbles.

### C. Formation of gas-rich layer

We have found that two neighboring surface nanobubbles can merge into a large nanobubble. It also turns out that the two neighboring surface nanobubbles can form a gas-rich layer under certain conditions. Such a gas-rich layer between interacting solid and liquid plays a very important role in more effectively weakening the solid-liquid interaction, leading to a greater reduction in drag. Recently, Hu *et al.* proposed a novel design incorporating alternating superhydrophobic and hydrophilic strips that can form stable and continuous air rings [1]. Here, we further investigate the conditions for the formation of a gas-rich layer. We suggest that two neighboring surface nanobubbles can either merge into a large nanobubble or form a gas-rich layer, depending on the values of the surface nanobubble saturation ($N_{\text{nanobubble}}/N_{\text{total}}$) and the ratio of solid-gas to solid-liquid interaction strengths ($\varepsilon_{sg}/\varepsilon_{sl}$). It can be seen from Fig. 8(a) that for weak solid-gas interaction (e.g., $\varepsilon_{sg}/\varepsilon_{sl} = 1.176$), a higher gas saturation (about 92%) in the nanobubble is required in order that two neighboring surface nanobubbles can form a gas-rich layer on the solid substrate. It is interesting to find that two neighboring surface nanobubbles can still form a gas-rich layer at a gas saturation of only 7.6%, as long as the interaction between the solid and the gas is sufficiently strong ($\varepsilon_{sg}/\varepsilon_{sl} = 1.538$). The gas-rich layer thus formed continually absorbs gas molecules around it until saturation (ripening) is reached. Figure 8(b) shows the shape of the gas-rich layer, which is very similar to that of the air rings that have been observed in experimental studies [1]. In this diagram, $w$ is the axial thickness of the gas-rich layer, $h$ is the gas-rich layer height, and $\theta$ is the contact angle.

MD simulations reveal directly that the gas molecules inside and outside the nanobubbles are exchanged continuously. Therefore, a gas-rich layer can form as a result of transfer of gas molecules from one surface nanobubble to another along the solid substrate. The mechanism is similar to that

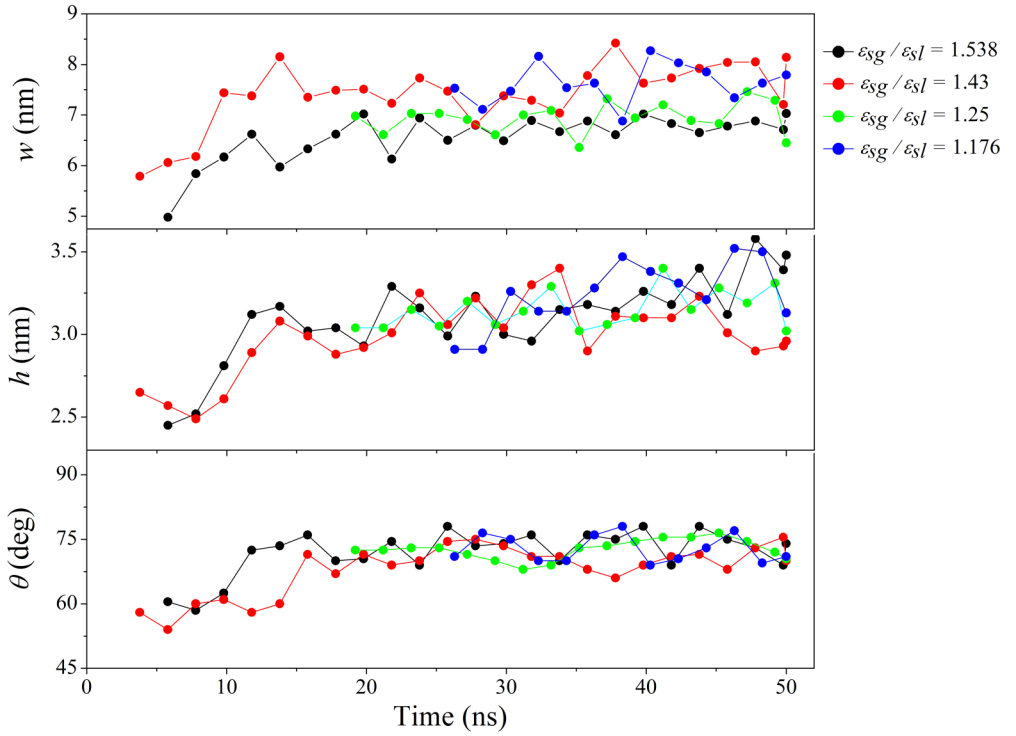


FIG. 9. Variation of the shape of the gas-rich layer with time for different values of $\varepsilon_{sg}/\varepsilon_{sl}$ ($w$ is the axial thickness of the gas-rich layer, $h$ is the gas-rich layer height, and $\theta$ is the contact angle).

involved in the coalescence of two nanobubbles, but, because of strong solid-gas interaction, the gas molecules that flow out of one surface nanobubble no longer pass into another surface nanobubble, but instead remain on the solid surface and connect with both nanobubbles, inducing the formation of the gas-rich layer.

As mentioned earlier, a gas-rich layer can prevent direct liquid-solid contact, leading to maximization of energy efficiency and reduction of drag for underwater vehicles. Some studies have also demonstrated that the shape of the gas-rich layer plays a crucial role in drag reduction [1,24]. Therefore, we also investigated the evolution of the shape of the gas-rich layer (in terms of $w$, $h$, and $\theta$) as a function of time for different values of the ratio of $\varepsilon_{sg}/\varepsilon_{sl}$, as shown in Fig. 9. The contact angle was obtained by fitting the gas-rich layer profile as circular arcs. When $\varepsilon_{sg}/\varepsilon_{sl} > 1.43$, the gas-rich layer initially has small values of $w$ and $h$ although it still continuously absorbs gas molecules from the bulk liquid. For strong gas-solid interaction ($\varepsilon_{sg}/\varepsilon_{sl} = 1.538$), the axial thickness $w$ of the gas-rich layer, which is critical for drag reduction, remains almost stable after the gas-rich layer reaches saturation at about 22 ns. The increase in the height $h$ and contact angle $\theta$ of the gas-rich layer is not linearly proportional to the gas-solid interaction strength.

## IV. CONCLUSIONS

At a fixed gas concentration, the size of bulk nanobubbles can be effectively controlled by varying the ratio of gas-gas to liquid-gas interaction strengths ($\varepsilon_{gg}/\varepsilon_{gl}$). Increasing $\varepsilon_{gg}/\varepsilon_{gl}$ leads to the formation of large bulk nanobubbles in the bulk liquid. Small bulk nanobubbles usually dissolve through outflow of gas molecules. However, they can also remain stable in bulk liquid, as long as the ratio of solid-gas to liquid-gas interaction strength is sufficiently high. Two neighboring surface nanobubbles exhibit two types of dynamic behavior, depending on the relative gas-liquid-solid

interaction strengths. In the absence of contact line pinning, they can merge directly to form a larger surface nanobubble; alternatively, one nanobubble can grow at the expense of the other. In addition to gas-liquid-solid interactions, both differences in relative size and the distance between two surface nanobubbles are critical in determining the interaction behavior of two neighboring surface nanobubbles. It is interesting to find that two neighboring unsaturated surface nanobubbles can also form a gas-rich layer, as long as the solid-gas interaction is sufficiently strong. Moreover, the axial thickness of the gas-rich layer can remain stable, provided that the gas-solid interaction is stronger than the liquid-solid interaction. However, the height of the gas-rich layer and the contact angle are not linearly proportional to the gas-solid and liquid-solid interaction strength. We hope that our results could serve as a reference to help in developing potential applications of nanobubbles.

## ACKNOWLEDGMENTS

This work was supported by the Fundamental Research Funds for the Central Universities (Grant No. HEUCFG201711), and the Natural Science Foundation of Heilongjiang Province, China (Grant No. JJ2017ZR0691).

[1] H. Hu, J. Wen, L. Bao, L. Jia, D. Song, B. Song, G. Pan, M. Scaraggi, D. Dini, Q. Xue, and F. Zhou, Significant and stable drag reduction with air rings confined by alternated superhydrophobic and hydrophilic strips, Sci. Adv. **3**, 1603288 (2017).

[2] S. L. Ceccio, Friction drag reduction of external flows with bubble and gas injection, Annu. Rev. Fluid Mech. **42**, 183 (2010).

[3] J. P. Rothstein, Slip on superhydrophobic surface, Annu. Rev. Fluid Mech. **42**, 89 (2010).

[4] B. R. Elbing, S. Makiharju, A. Wiggins, M. Perlin, D. R. Dowling, and S. L. Ceccio, On the scaling of air layer drag reduction, J. Fluid Mech. **717**, 484 (2013).

[5] B. R. Elbing, E. S. Winkel, K. A. Lay, S. L. Ceccio, D. R. Dowling, and M. Perlin, Bubble-induced skin-friction drag reduction and the abrupt transition to air-layer drag reduction, J. Fluid Mech. **612**, 201 (2008).

[6] Y. Murai, H. Oiwa, and Y. Takeda, Frictional drag reduction in bubbly Couette-Taylor flow, Phys. Fluids **20**, 034101 (2008).

[7] W. C. Sanders, E. S. Winkel, D. R. Dowling, M. Perlin, and S. L. Ceccio, Bubble friction drag reduction in a high-Reynolds-number flat-plate turbulent boundary layer, J. Fluid Mech. **552**, 353 (2006).

[8] T. H. van den Berg, S. Luther, D. P. Lathrop, and D. Lohse, Drag Reduction in Bubbly Taylor-Couette Turbulence, Phys. Rev. Lett. **94**, 044501 (2005).

[9] M. Zhang and J. R. T. Seddon, Nanobubble-nanoparticle interactions in bulk solutions, Langmuir **32**, 11280 (2016).

[10] C. Li, A. M. Zhang, S. Wang, and P. Cui, Formation and coalescence of nanobubbles under controlled gas concentration and species, AIP Adv. **8**, 015104 (2018).

[11] J. H. Weijs, J. H. Snoeijer, and D. Lohse, Formation of Surface Nanobubbles and the Universality of Their Contact Angles: A Molecular Dynamics Approach, Phys. Rev. Lett. **108**, 104501 (2012).

[12] J. H. Weijs and D. Lohse, Why Surface Nanobubbles Live for Hours, Phys. Rev. Lett. **110**, 054501 (2013).

[13] S. Maheshwari, M. van der Hoef, X. Zhang, and D. Lohse, Stability of surface nanobubbles: a molecular dynamics study, Langmuir **32**, 11116 (2016).

[14] J. Wei, X. Zhang, and F. Song, Deformation of surface nanobubbles induced by substrate hydrophobicity, Langmuir **32**, 13003 (2016).

[15] S. Maheshwari, M. van der Hoef, J. R. Rodriguez, and D. Lohse, Leakiness of pinned neighboring surface nanobubbles induced by strong gas-surface interaction, ACS Nano **12**, 2603 (2018).

[16] X. Zhu, R. Verzicco, X. Zhang, and D. Lohse, Diffusive interaction of multiple surface nanobubbles: shrinkage, growth, and coarsening, Soft Matter **14**, 2006 (2018).

[17] B. Bhushan, Y. Wang, and A. Maali, Coalescence and movement of nanobubbles studied with tapping mode AFM and tip-bubble interaction analysis, J. Phys.: Condens. Matter **20**, 485004 (2008).
[18] D. Li, D. Jing, Y. Pan, W. Wang, and X. Zhao, Coalescence and stability analysis of surface nanobubbles on the polystyrene/water interface, Langmuir **30**, 6079 (2014).
[19] J. B. Park, D. Shin, S. Kang, S. P. Cho, and B. H. Hong, Distortion in two-dimensional shapes of merging nanobubbles: evidence for anisotropic gas flow mechanism, Langmuir **32**, 11303 (2016).
[20] D. Lohse and X. Zhang, Surface nanobubbles and nanodroplets, Rev. Mod. Phys. **87**, 981 (2015).
[21] B. Dollet and D. Lohse, Pinning stabilizes neighboring surface nanobubbles against Ostwald ripening, Langmuir **32**, 11335 (2016).
[22] B. Hess, C. Kutzner, D. van der Spoel, and E. Lindahl, GROMACS 4: Algorithms for highly efficient, load-balanced, and scalable molecular simulation, J. Chem. Theory Comput. **4**, 435 (2008).
[23] G. Menzl, M. A. Gonzalez, P. Geiger, F. Caupin, J. L. F. Abascal, C. Valeriani, and C. Dellago, Molecular mechanism for cavitation in water under tension, Proc. Natl. Acad. Sci. USA **113**, 13582 (2016).
[24] E. Aljallis, M. A. Sarshar, R. Datla, V. Sikka, A. Jones, and C. H. Choi, Experimental study of skin friction drag reduction on superhydrophobic flat plates in high Reynolds number boundary layer flow, Phys. Fluids **25**, 025103 (2013).